Adsorption, Activation, and Dissociation of Oxygen on Doped Oxides**

Yi Cui, Xiang Shao, Matthias Baldofski, Joachim Sauer, Niklas Nilius, and Hans-Joachim Freund*

Dedicated to Professor Helmut Schwarz on the occasion of his 70th birthday

The activation of small molecules is one of the key issues in heterogeneous catalysis.[1] Common diatomic species, such as O_2, H_2 and N_2, are chemically inert and require activation at elevated temperature and pressure. The associated barriers can be lowered with catalytically active metals that alter the stability of the molecules by electron transfer into their antibonding orbitals. Also reducible oxides offer suitable sites for molecular activation, such as surface O vacancies.[2] Wide-band-gap materials, on the other hand, are unable to bind small molecules due to a high degree of surface saturation. Molecular activation can still be achieved if dopants are introduced into the host lattices.[3] While low-valence impurities reduce the formation energy of O vacancies,[4,5] which are then available for binding molecular species,[6–9] high-valence dopants may directly activate an adsorbate by electron transfer.[10] Against common perception, molecular activation on doped oxides does not require any structural defects, a condition that renders this mechanism interesting for high-temperature applications in which surface irregularities typically heal on short time scales. One model reaction in which dopants may play a pivotal role for the molecular activation is the oxidative coupling of methane that only runs at temperatures above 1000 K.[11,12]

The strong effect of donor-type impurities was recently demonstrated for Mo-doped CaO films.[13] When gold was deposited on such films at room temperature, only monolayer islands were observed on the surface. This unusual growth behavior was attributed to a charge transfer from the Mo dopants to the adsorbed gold, giving rise to a substantial increase of the metal–oxide adhesion.[14] Herein we show that dopant-induced charge transfer is relevant also for the adsorption and activation of small molecules such as O_2. Using scanning tunneling microscopy (STM) and density functional theory (DFT), we provide evidence that strongly bound O_2^- species with high susceptibility for dissociation form even on chemically inert CaO(001) after it has been doped with Mo ions.

Figure 1 displays STM images of atomically flat, doped CaO(001) films before and after exposure to O_2. In empty-state images, the adspecies appear as circular depressions 0.6 Å in depth and 10 Å in diameter. Exposing them to electrons from the STM tip reveals their molecular nature, as

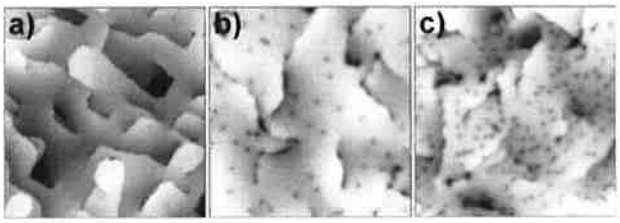

Figure 1. STM images of a) a pristine 25-monolayer CaO(001) film (4.0 V, 80×80 nm^2) and b) films after O_2 exposure of 5 L at 20 K and c) 200 L at 300 K (40×40 nm^2).

the adsorbates split into pairs of identical minima that are assigned to the respective O atoms (Figure 2).[15] Whereas a mean O–O distance of 10–15 Å is observed directly after dissociation, this number increases with time due to the repulsive character of the O–O interaction on the surface. The two types of oxygen species can be distinguished also in bias-dependent topographic images (Figure 2c). While the molecules show pronounced negative contrast, the atomic species appear fainter and are surrounded by a bright halo.

The adsorption efficiency of oxygen strongly depends on the preparation of the CaO films, in particular on the concentration of the Mo dopants. This becomes evident in Figure 3, which displays weakly and strongly doped CaO films after exposure to 5 L O_2 at 20 K. Whereas Mo-poor films are unable to bind oxygen, an adsorbate concentration of roughly 10^{17} m^{-2} is found for Mo-rich preparations, indicating the crucial role of the dopants for binding. To correlate the Mo concentration with the CaO reactivity towards oxygen, we use

[*] Dr. Y. Cui,[+] Dr. X. Shao,[++][+] Dr. N. Nilius, Prof. H.-J. Freund
Abteilung Chemische Physik
Fritz-Haber-Institut der Max-Planck-Gesellschaft
Faradayweg 4–6, 14195 Berlin (Germany)
E-mail: nilius@fhi-berlin.mpg.de
Dr. N. Nilius
Institut für Physik
Carl von Ossietzky Universität Oldenburg
26111 Oldenburg (Germany)
Dipl.-Chem. M. Baldofski, Prof. J. Sauer
Institut für Chemie, Humboldt-Universität zu Berlin
Unter den Linden 6, 10099 Berlin (Germany)
[++] Present address: Department of Chemical Physics
University of Science & Technology
Hefei 230026 (China)
[+] These authors contributed equally to this work.
[**] We thank the DFG for financial support within the Excellence Cluster "UniCat" and the Humboldt Foundation (fellowship to Y.C.).

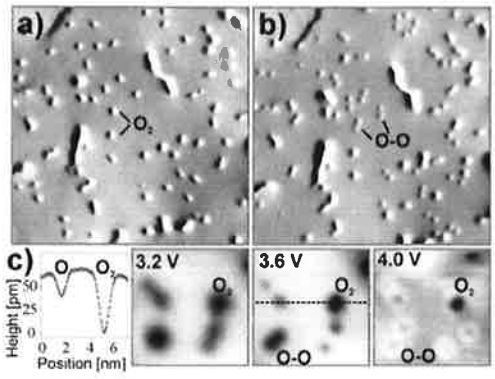

Figure 2. STM images of the same O_2-covered region of Mo-doped CaO recorded a) before and b) after multiple scans at 4.0 V (3.3 V, 40×40 nm²). Note that most molecules have dissociated into atom pairs upon electron injection from the tip. c) Height profile and bias-dependent contrast of oxygen molecules and atoms. While atoms appear with bright halos at higher bias, the molecules are imaged as deep depressions in the surface.

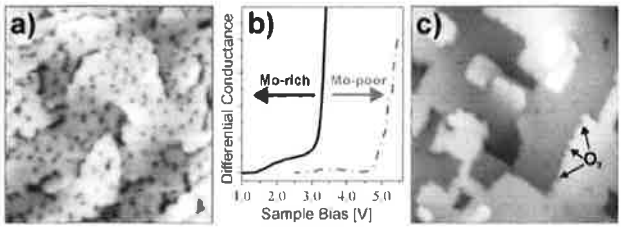

Figure 3. a,c) STM images of strongly and weakly doped CaO films after exposure to 5 L O_2 at 20 K (40×40 nm²). The O_2 adsorption probability correlates with the position of the CaO conduction band, as measured with STM conductance spectroscopy (b). Step edges are preferred O_2 binding sites only on weakly doped films (see arrows in c).

the position of the oxide conduction band with respect to the Fermi level as a descriptor. With increasing donor concentration in the matrix, the band position experiences a downshift, as electrons are transfered from interfacial Mo species to the metal substrate below.[16] This charge flow generates a positive interface dipole between oxide film and metal support that shifts the vacuum level and, closely related, the oxide conduction band to lower energy (Figure 3b).

We now observe a steep onset in the O_2 adsorption probability when the band edge drops below 3.0 eV, while films with a band position higher than 4.0 eV are unable to bind oxygen. Again, electron donation from the Mo impurities seems to be the crucial requirement for molecular activation.

Although the band position is a nonlocal parameter, we believe that dopants and O_2 molecules interact directly with each other and not through a delocalized charge background. Experimental evidence comes from O_2 desorption experiments, in which isolated molecules are removed from the surface by a bias pulse with the tip (Figure 4). In 50% of these experiments, a Mo donor is detected below the molecule. Interestingly, the dopant never occupies a position directly in the top layer but sits in sub-surface oxide planes, as deduced

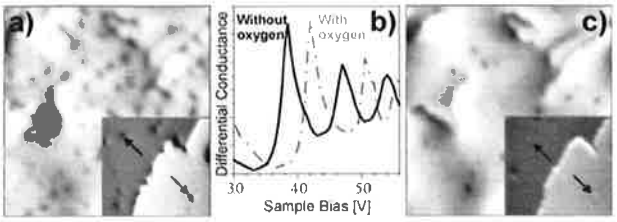

Figure 4. a,c) Identical CaO region before and after O_2 desorption with the tip (3.3 V, 27×27 nm²). The inset shows a selected area at higher resolution, revealing characteristic ring structures below the O_2 molecules (see arrows). These rings are the charging fingerprints of Mo dopants in a near-surface region (4.0 V, 17×17 nm²).[17] b) STM conductance spectra showing the downshift of CaO vacuum states after O_2 desorption from the surface.

from the diameter of characteristic charging rings emerging in the STM images (see the Supporting Information and Ref. [17] for details). We conclude that the Mo ions are able to exchange charges with the surface O_2 molecules even over distances as large as 1 nm, for example, by means of electron tunneling.

The formation of superoxo (O_2^-) species on the surface of Mo-doped CaO is corroborated by spectroscopic techniques. In XPS, we find a downward shift of Ca(2p) and O(1s) binding energies by roughly 0.2 eV after dosing O_2 onto the films. The same trend is observed for the band positions determined with STM conductance spectroscopy (see the Supporting Information). Both shifts indicate a workfunction increase $\Delta\phi$ due to the electron transfer into the adsorbates. The amount of charge transfer can be quantified directly by measuring $\Delta\phi$ after desorbing the O_2^- species from a given surface region and monitoring the associated shift of the vacuum states with STM spectroscopy (Figure 4b).[18] We find a rigid downshift of all states by 0.35 eV (workfunction reduction), which is explained by the removal of vertical $Mo^{\delta+}$–$O_2^{\delta-}$ dipoles upon oxygen desorption. The Helmholtz formula $\Delta\varphi = \frac{\varepsilon}{\varepsilon_0 \varepsilon_{CaO}} \mu_{ad} N_{ad}$ allows us to connect $\Delta\phi$ with the dipole strength μ_{ad} of the charge-transfer pairs. For an O_2 surface density of $N_{ad} = 10^{17}\ m^{-2}$ and a dielectric constant of $\varepsilon_{CaO} = 10$, we calculate a dipole moment of 3×10^{-28} C m, which is compatible with the transfer of one electron from a Mo ion in the sixth subsurface plane to a surface O_2. The last hint for O_2^- formation on doped CaO films comes from the facile dissociation of the molecules, which proceeds with close to 100% probability when 4.0 V electrons are injected from the tip (1 min at 20 pA). The bond cleavage occurs as another electron enters the antibonding states of the already weakened superoxo species.

The electron transfer between Mo donors and O_2 acceptors has been reproduced with DFT calculations performed at the B3LYP + D level. On nondoped CaO(001), a neutral O_2 molecule binds with 13 kJ mol^{-1} (mostly from dispersion forces) to a Ca–Ca bridge position, while Ca^{2+} top sites are less preferred. In contrast, an O_2^- species binds to the same bridge site with a binding energy of 87 kJ mol^{-1} when a Mo^{3+} ion is present in the third subsurface plane. The charge transfer to oxygen becomes even more favorable for Mo^{2+} donors in the oxide film, given their low ionization energy.[13]

Further evidence for the formation of superoxo species comes from the bond elongation (121 to 133 pm) and the reduced stretching frequency (1537 to 1200 cm^{-1}) computed for O_2 molecules on the doped oxide. Moreover, the total spin of the system decreases from $^5/_2$ ($^3/_2$ for Mo^{3+} (d^3) plus $^2/_2$ for O_2) to $^3/_2$ ($^2/_2$ for Mo^{4+} (d^2) plus $^1/_2$ for O_2^-) in response to the charge transfer. And finally, we calculated a lower apparent dissociation barrier for superoxo species on doped CaO (66 kJ mol^{-1}) compared to that of neutral O_2 on pristine CaO (110 kJ mol^{-1}), following the trend observed experimentally. Further details on the nature of the superoxo species can be found in the Supporting Information.

In summary, we have shown that O_2 molecules may be activated to form superoxo species even on smooth, defect-free surfaces of nonreducible oxides when dopants are present in the bulk. The O_2^- on Mo-doped CaO is bound with an energy of roughly 90 kJ mol^{-1}, and is hence stable at room temperature. Moreover, the species is prone to dissociation into atomic oxygen on the doped surface. We conclude that dopants may play a pivotal role in the activation of hydrocarbons on wide-band-gap oxides, and refer to a corresponding paper from the Schlögl group on this issue which demonstrates an unusually high reaction yield for the oxidative coupling of methane on an Fe-doped MgO powder sample.[12]

Experimental Section

CaO films were grown on Mo(001) by deposition of elemental Ca in 5×10^{-7} mbar O_2 and annealing at 1000 K in vacuum. The films are characterized by a square (1 × 1) LEED pattern, indicative of the (001) termination of the CaO surface, and by flat terraces of approximately 100 nm^2 in size in STM.[19] The CaO films are subject to self-doping, proceeding by spontaneous diffusion of Mo ions from the metal support into the film at elevated temperature.[20] While interfacial oxide planes contain up to 25% Mo ions, this number decreases with increasing film thickness. A desired Mo concentration in a near-surface region of the film can be obtained by varying the thickness and the annealing temperature, the latter promoting Mo diffusion. The Mo concentration was estimated either from XPS, from the number of near-surface impurities seen in STM, or from the position of the CaO conduction band in STM conductance spectroscopy.

Computational approach: The DFT calculations were performed with PBE[21] and B3LYP[22] exchange-correlation functionals and a TZVP basis set.[23] The Mo core electrons are described by the Hay–Wadt effective core potential.[24] Dispersion was added as a damped summation over $1/r^6$ atom–atom terms using the Grimme parameterization.[25] We used $Ca_{34}O_{34}$ cluster models, surrounded by a shell of full-ion effective core potentials on Ca^{2+} positions and embedded into a periodic array of point charges.[26]

Received: June 14, 2013
Published online: September 17, 2013

Keywords: dopants · heterogeneous catalysis · oxidation · oxygen activation · surface chemistry

[1] G. Ertl, H. Knoezinger, F. Schueth, J. Weitkamp, *Handbook of heterogeneous catalysis*, Wiley-VCH, Weinheim, **2008**.
[2] G. N. Vayssilov, Y. Lykhach, A. Migani, T. Staudt, G. P. Petrova, N. Tsud, T. Skala, A. Bruix, F. Illas, K. C. Prince, V. Matolin, K. M. Neyman, J. Libuda, *Nat. Mater.* **2011**, *10*, 310.
[3] E. W. McFarland, H. Metiu, *Chem. Rev.* **2013**, 113, 4391; Z. P. Hu, B. Li, X. Y. Sun, H. Metiu, *J. Phys. Chem. C* **2011**, *115*, 3065.
[4] H. Y. Kim, H. M. Lee, R. G. S. Pala, V. Shapovalov, H. Metiu, *J. Phys. Chem. C* **2008**, *112*, 12398.
[5] P. Myrach, N. Nilius, S. V. Levchenko, A. Gonchar, T. Risse, K. P. Dinse, L. A. Boatner, W. Frandsen, R. Horn, H. J. Freund, R. Schlogl, M. Scheffler, *ChemCatChem* **2010**, *2*, 854.
[6] M. A. Henderson, W. S. Epling, C. L. Perkins, C. H. F. Peden, U. Diebold, *J. Phys. Chem. B* **1999**, *103*, 5328.
[7] L. M. Molina, B. Hammer, *Appl. Catal. A* **2005**, *291*, 21.
[8] N. G. Petrik, Z. Zhang, Y. Du, Z. Dohnálek, I. Lyubinetsky, G. A. Kimmel, *J. Phys. Chem. C* **2009**, *113*, 12407.
[9] Z. Zhang, J. T. Yates, *J. Am. Chem. Soc.* **2010**, *132*, 12804.
[10] A. Gonchar, T. Risse, H.-J. Freund, L. Giordano, C. Di Valentin, G. Pacchioni, *Angew. Chem.* **2011**, *123*, 2684; *Angew. Chem. Int. Ed.* **2011**, *50*, 2635.
[11] J. H. Lunsford, *Angew. Chem.* **1995**, *107*, 1059; *Angew. Chem. Int. Ed. Engl.* **1995**, *34*, 970.
[12] P. Schwach, A. Trunschke, R. Schlögl, *Angew. Chem.* **2013**, DOI: 10.1002/ange.201305470; *Angew. Chem. Int. Ed.* **2013**, DOI: 10.1002/anie.201305470.
[13] X. Shao, S. Prada, L. Giordano, G. Pacchioni, N. Nilius, H. J. Freund, *Angew. Chem.* **2011**, *123*, 11728; *Angew. Chem. Int. Ed.* **2011**, *50*, 11525.
[14] J. Andersin, J. Nevalaita, K. Honkala, H. Hakkinen, *Angew. Chem.* **2013**, *125*, 1464; *Angew. Chem. Int. Ed.* **2013**, *52*, 1424.
[15] B. C. Stipe, M. A. Rezaei, W. Ho, S. Gao, M. Persson, B. I. Lundqvist, *Phys. Rev. Lett.* **1997**, *78*, 4410.
[16] X. Shao, N. Nilius, H. J. Freund, *J. Am. Chem. Soc.* **2012**, *134*, 2532.
[17] Y. Cui, N. Nilius, H. J. Freund, S. Prada, L. Giordano, G. Pacchioni, unpublished results.
[18] G. Binnig, K. H. Frank, H. Fuchs, N. Garcia, B. Reihl, H. Rohrer, F. Salvan, A. R. Williams, *Phys. Rev. Lett.* **1985**, *55*, 991.
[19] X. Shao, P. Myrach, N. Nilius, H. J. Freund, *J. Phys. Chem. C* **2011**, *115*, 8784.
[20] X. Shao, N. Nilius, P. Myrach, H. J. Freund, U. Martinez, S. Prada, L. Giordano, G. Pacchioni, *Phys. Rev. B* **2011**, *83*, 245407.
[21] J. P. Perdew, K. Burke, M. Ernzerhof, *Phys. Rev. Lett.* **1996**, *77*, 3865.
[22] A. D. Becke, *J. Chem. Phys.* **1993**, *98*, 5648; C. Lee, W. Yang, R. G. Parr, *Phys. Rev. B* **1988**, *37*, 785.
[23] F. Weigend, R. Ahlrichs, *Phys. Chem. Chem. Phys.* **2005**, *7*, 3297.
[24] W. R. Wadt, P. J. Hay, *J. Chem. Phys.* **1985**, *82*, 270.
[25] S. Grimme, *J. Comput. Chem.* **2006**, *27*, 1787.
[26] A. M. Burow, M. Sierka, J. Döbler, J. Sauer, *J. Chem. Phys.* **2009**, *130*, 174710.